

**Pressure induced valence change of Eu in EuFe<sub>2</sub>As<sub>2</sub> at low temperature and high pressures probed by resonant inelastic x-ray scattering**

Ravhi S. Kumar, Yi Zhang, Arumugam Thamizhavel, A. Svane, G. Vaitheeswaran, V. Kanchana, Yuming Xiao, Paul Chow, Changfeng Chen, and Yusheng Zhao

Citation: *Applied Physics Letters* **104**, 042601 (2014); doi: 10.1063/1.4863203

View online: <http://dx.doi.org/10.1063/1.4863203>

View Table of Contents: <http://scitation.aip.org/content/aip/journal/apl/104/4?ver=pdfcov>

Published by the [AIP Publishing](#)

---

**Articles you may be interested in**

Soft x-ray magnetic circular dichroism study of valence and spin states in FeT<sub>2</sub>O<sub>4</sub> (T=V, Cr) spinel oxides  
*J. Appl. Phys.* **113**, 17E116 (2013); 10.1063/1.4793769

Competition of 3d/4f orbitals due to competing conductivity and ferromagnetism in Fe/CoAs layers in Eu(Fe<sub>0.89</sub>Co<sub>0.11</sub>)<sub>2</sub>As<sub>2</sub>  
*J. Appl. Phys.* **113**, 013907 (2013); 10.1063/1.4772760

Electronic structure and characteristics of Fe 3d valence states of Fe<sub>1.01</sub>Se superconductors under pressure probed by x-ray absorption spectroscopy and resonant x-ray emission spectroscopy  
*J. Chem. Phys.* **137**, 244702 (2012); 10.1063/1.4772466

Magnetic properties of single crystal EuCo<sub>2</sub>As<sub>2</sub>  
*J. Appl. Phys.* **111**, 07E106 (2012); 10.1063/1.3671410

Thermally activated charge transfer in a Prussian blue derivative probed by resonant inelastic x-ray scattering  
*Appl. Phys. Lett.* **93**, 054101 (2008); 10.1063/1.2966355

---

An advertisement for the journal 'Computing' in Science & Engineering. The image shows several tablets displaying the journal cover, which features a colorful, abstract pattern. The text 'computing' is written in a stylized font, with 'SCIENCE & ENGINEERING' underneath. Below the image, the text reads 'AIP's JOURNAL OF COMPUTATIONAL TOOLS AND METHODS. AVAILABLE AT MOST LIBRARIES.'

**computing**  
SCIENCE & ENGINEERING

AIP's JOURNAL OF COMPUTATIONAL TOOLS AND METHODS.  
**AVAILABLE AT MOST LIBRARIES.**

## Pressure induced valence change of Eu in $\text{EuFe}_2\text{As}_2$ at low temperature and high pressures probed by resonant inelastic x-ray scattering

Ravhi S. Kumar,<sup>1,a)</sup> Yi Zhang,<sup>1</sup> Arumugam Thamizhavel,<sup>2</sup> A. Svane,<sup>3</sup> G. Vaitheeswaran,<sup>4</sup> V. Kanchana,<sup>5</sup> Yuming Xiao,<sup>6</sup> Paul Chow,<sup>6</sup> Changfeng Chen,<sup>1</sup> and Yusheng Zhao<sup>1</sup>

<sup>1</sup>Department of Physics and High Pressure Science and Engineering Centre, University of Nevada Las Vegas, 4505 Maryland Parkway, Las Vegas, Nevada 89154, USA

<sup>2</sup>Department of Condensed Matter Physics and Materials Science, Tata Institute of Fundamental Research, Homi Bhabha Road, Colaba, Mumbai 400 005, India

<sup>3</sup>Department of Physics and Astronomy, Aarhus University, DK-8000 Aarhus C, Denmark

<sup>4</sup>Advanced Centre of Research in High Energy Materials (ACRHEM), University of Hyderabad, Hyderabad 500 046, Andhra Pradesh, India

<sup>5</sup>Department of Physics, Indian Institute of Technology Hyderabad, Ordnance Factory Estate, Yeddumailaram 502 205, Andhra Pradesh, India

<sup>6</sup>HPCAT, Geophysical Laboratory, Carnegie Institution of Washington, Advanced Photon Source, Argonne National Laboratory, Argonne, Illinois 60439, USA

(Received 13 November 2013; accepted 10 January 2014; published online 27 January 2014)

The effect of pressure on the valence state of Eu in  $\text{EuFe}_2\text{As}_2$  has been investigated at high pressures up to 43 GPa at 10 K using resonant inelastic x-ray scattering and x-ray absorption spectroscopy using partial fluorescence yield. Two distinct density functional approaches have been used to complement the experiments. Our experimental results show that the Eu valence increases from a divalent state to a nearly trivalent state under application of pressure in consistence with theoretical simulations. Furthermore, our calculations show that the Eu magnetic moments prevail at high pressure up to 45 GPa. © 2014 AIP Publishing LLC.

[<http://dx.doi.org/10.1063/1.4863203>]

Discovery of iron based superconductors with transition temperature ( $T_c$ ) up to 56 K in the so called “1111” compounds,  $\text{RFeAsO}$  (R = Lanthanide such as La, Ce, Sm, and Gd) and  $T_c$  up to 38 K in “122” compounds,  $\text{AFe}_2\text{As}_2$  (A = Ca, Sr, Eu, and Ba) has drawn tremendous attention in recent years.<sup>1–4</sup>  $\text{EuFe}_2\text{As}_2$  is the only rare earth member of the 122 class of compounds and exhibits a superconducting transition temperature  $T_c$  of around 28 K under application of pressure above 2.5 GPa.<sup>5,6</sup> At ambient conditions, the compound is in a paramagnetic state with a tetragonal  $\text{ThCr}_2\text{Si}_2$  type structure. It further undergoes an orthorhombic structural transition together with a spin density wave (SDW) type antiferromagnetic ordering at 190 K.<sup>7–10</sup> Application of pressure suppresses the SDW and Neel temperature and favors the charge transfer between the insulating and conducting layers. Furthermore, pressure not only influences the important parameters correlated to the  $T_c$  such as crystal structure, magnetic and spin ordering of the system but also alters the valence which is another important parameter affecting the  $T_c$ . Here, we report an investigation of the Eu valence in  $\text{EuFe}_2\text{As}_2$  for pressures up to 43 GPa and at low temperature, where superconductivity appears on application of pressure. Resonant Inelastic X-ray Scattering (RIXS) measurements are bulk sensitive and constitute an excellent probe to determine valence changes under extreme conditions.<sup>11–13</sup> Our experiments and calculations show that the Eu valence sharply increases on application of pressure to a nearly trivalent state above 9 GPa at 10 K. Further, this

sharp increase in valence is found to occur around the critical pressure where a structural transition to a collapsed tetragonal (CT) phase is observed.

Single crystals of  $\text{EuFe}_2\text{As}_2$  were grown by using Sn through flux technique with starting composition Eu:Fe:As:Sn in the ratio 1:2:2:19. The Sn was removed by centrifugal method. The grown crystals were characterized by Energy Dispersive Analysis of X-rays (EDAX), resistivity, specific heat, and magnetic susceptibility as reported elsewhere.<sup>10</sup> A small crystal is selected from the batch and loaded into a 125  $\mu\text{m}$  hole drilled in a Be gasket pre-indented to 40  $\mu\text{m}$  with a ruby sphere in a symmetric type diamond anvil cell using He as pressure transmitting medium. RIXS and Partial Fluorescence Yield (PFY) experiments were performed at Sector 16 ID-D of the Advanced Photon Source by focusing the incident x-ray beam to  $20 \times 50 \mu\text{m}^2$  (V  $\times$  H). The incident energy was set at the Eu  $L_3$  absorption edge, where the signal from the sample was analyzed by a spherically bent Si single crystal and an AmpTek detector in a Rowland circle. The total energy resolution in our experiments is 1 eV. First principle calculations presented in this work are performed using the Perdew-Burke-Ernzerhof generalized gradient approximation (GGA) as implemented in the VASP code.<sup>6</sup> We used the projector augmented plane wave (PAW) pseudopotential method with a plane wave basis and a cutoff energy of 400 eV. We have included the strong Coulomb repulsion in the Eu-4f orbital using the GGA + U approximation. The standard U of 8 eV for the  $\text{Eu}^{2+}$  ion is chosen in the calculation. The results with different U values have been tested for consistency. The self-interaction corrected local spin density (SIC-LSD) approximation<sup>13–16</sup> has been used to calculate the

<sup>a)</sup>Author to whom correspondence should be addressed. Electronic mail: ravhi@physics.unlv.edu. Tel.: +01 702 895 3228. FAX: +01 702 895 0804.

effective Eu valence, similar to the previous applications to Yb compounds.<sup>12,13</sup> The SIC-LSD method was implemented with the linear muffin-tin orbital method<sup>17</sup> using the atomic spheres approximation, by which the crystal volume is split into slightly overlapping spheres centered on the nuclear positions. In these calculations, a ferro-magnetic ordering of Eu moments was adopted.

Figure 1 shows both the RIXS and the PFY spectra obtained for  $\text{EuFe}_2\text{As}_2$  around 10 K at representative pressures. Two distinct peaks, observed around 6.975 keV and 6.983 keV in the PFY spectra, represent the 4f electron configuration for  $\text{Eu}^{2+}$  ( $4f^7$ ) and  $\text{Eu}^{3+}$  ( $4f^6$ ). In the representative PFY spectra, above 9 GPa the  $2+$  peak intensity drops rapidly and a simultaneous increase of intensity of  $3+$  peak is observed. A gradual shift of intensities between the two peaks indicates the progressive change from divalent to trivalent state of Eu. The RIXS spectra collected at 1 GPa and 43 GPa at 10 K are shown in the upper panel. In the 1 GPa

spectrum, the  $2+$  contribution is predominant and could be observed around 6.975 keV, the same PFY peak energy where the  $2+$  intensity is high. At 43 GPa, the collected RIXS spectrum revealed separation of two branches of intensities corresponding to two different valence contributions. At each pressure, the average valence was estimated by substituting the integrated intensities of the  $2+$  and  $3+$  components at that pressure into the linearly interpolating expression:  $v = 2 + I(3+)/[I(2+) + I(3+)]$ , where  $I(2+)$  and  $I(3+)$  represent the  $2+$  and  $3+$  intensities, respectively.<sup>10–12</sup>

The effective valence thus extracted is plotted as function of pressure in Fig. 2(a). The Eu valence increases sharply above 10 GPa to a value of 2.55, then grows more gradually to 2.7 around 43 GPa. Thus, the Eu valence does not completely change into a trivalent state in the pressure range studied here. The Eu effective valence as calculated with the SIC-LSD method is illustrated in Fig. 2(b), which shows the valence change as function of pressure. The calculations

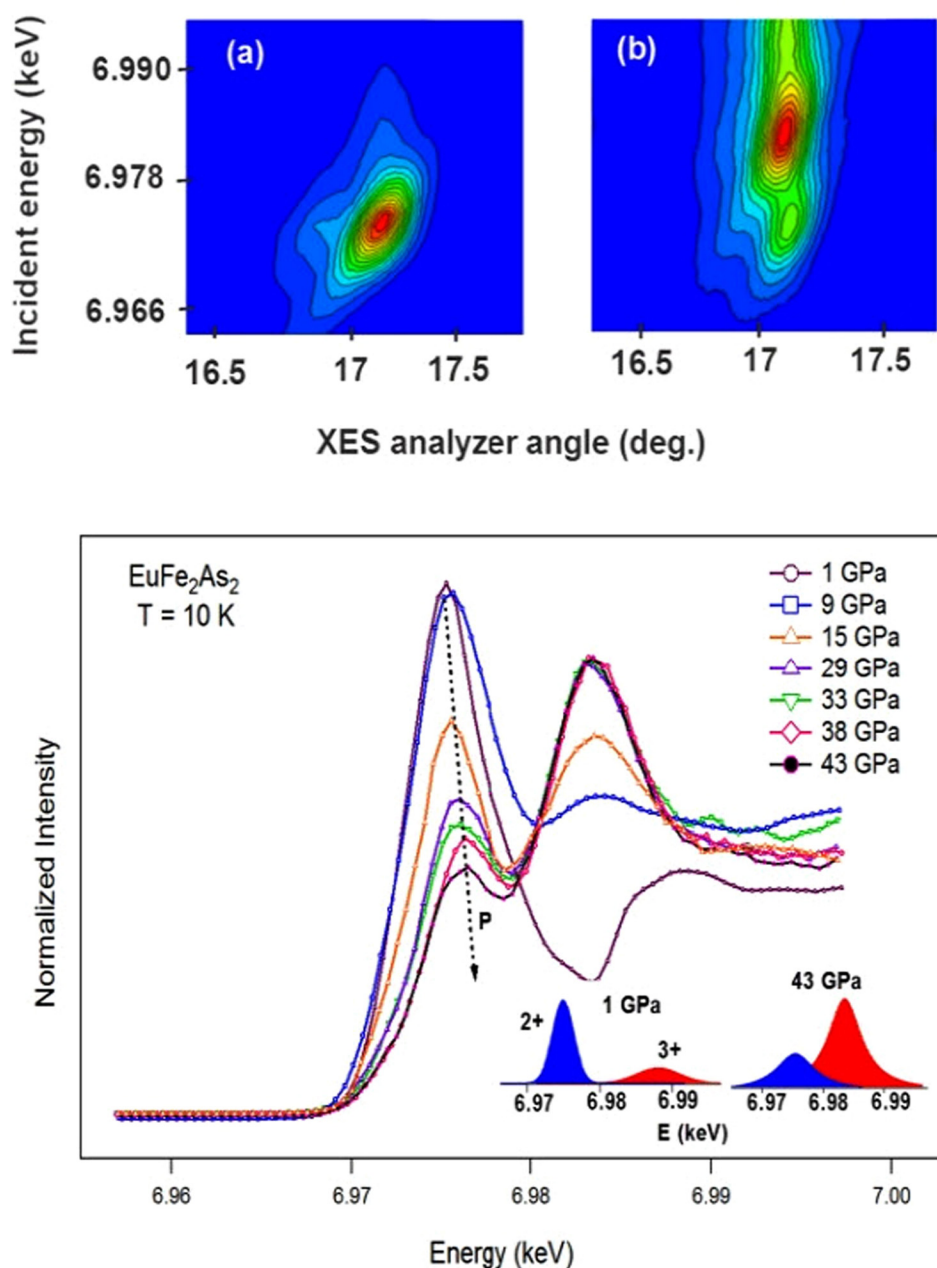


FIG. 1. X-ray absorption spectra collected in the PFY mode at 10 K up to 43 GPa. The inset shows the change in the intensity profile of divalent contribution as a function of pressure. The contour plot in the upper panel shows the RIXS spectra collected at (a) 1 GPa and (b) 43 GPa.

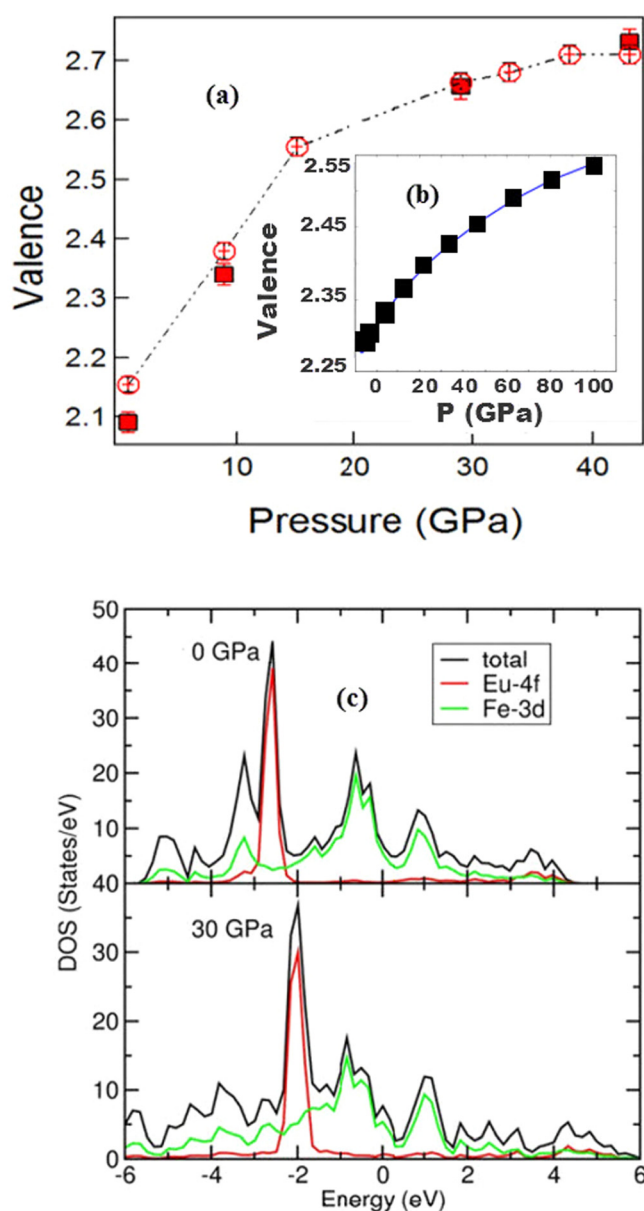


FIG. 2. (a) Pressure versus valence plot at 10 K for Eu in  $\text{EuFe}_2\text{As}_2$ . The open circles represent the data collected from the PFY measurements, and the filled squares represent the RIXS data. (b). Valence change as a function of pressure obtained by SIC-LSD calculations. (c). Calculated total and projected electron density of states of  $\text{EuFe}_2\text{As}_2$  at 0 and 30 GPa.

show a gradual shift from  $\text{Eu}^{2+}$  towards  $\text{Eu}^{3+}$ , which is at variance with the rapid change observed below 9 GPa, and more in line with the behavior observed at higher pressures.

The interplay between the crystal structure, the superconducting transition temperature  $T_c$ , and the Eu valence in  $\text{EuFe}_2\text{As}_2$  upon compression is of parametric importance. We may compare the transition pressure on valence changes observed in our experiments with the structural changes, superconductivity, and magnetic ordering reported under high pressures at low temperatures for  $\text{EuFe}_2\text{As}_2$ . The pressure-temperature phase diagram reported on  $\text{EuFe}_2\text{As}_2$  by Uhoya *et al.* shows that the  $I4/mmm$  tetragonal phase transforms into a CT phase around 9 GPa at ambient temperature.<sup>18</sup> A similar CT phase is also induced around 12 GPa when the low temperature orthorhombic phase is

compressed.<sup>18,19</sup> These experiments show that the CT phase is observed at high pressures at both low temperature and room temperature. The structural transition is however not associated with the pressure induced superconducting transition. The superconductivity phase diagram reported by Kurita *et al.* shows that the bulk superconductivity exists only in a narrow range of pressures from  $\sim 2.5$  GPa to 3.0 GPa.<sup>20</sup> Similar to external physical pressure, chemical pressure imparted in the system through doping also stabilizes the superconductivity in the 122 systems.<sup>21</sup> A further important observation is that application of pressure does not fully suppress the antiferromagnetic ordering, and the coexistence of superconductivity and magnetism prevails around 20 K. At higher pressures, above 8 GPa, the antiferromagnetic ordering changes to ferromagnetic, and  $\text{Eu}^{2+}$  magnetic moments remain up to high pressures above 20 GPa. A drastic Eu valence increase has been observed at 2 GPa by conventional x-ray absorption spectroscopy measurements (XAS) for tetragonal  $\text{EuFe}_2\text{As}_2$  at room temperature.<sup>22</sup> The valence reaches up to 2.33 and saturates around 9.8 GPa. However, the present experiments at low temperatures for the orthorhombic phase of  $\text{EuFe}_2\text{As}_2$  show a distinct change in valence evolution around 9 GPa. The valence increases rapidly up to 9 GPa and continues increasing more sluggishly up to the highest pressure, reaching a value around 2.7, i.e., a fully trivalent state is not reached even at pressures above 40 GPa. The slope change in the valence plot above 9 GPa observed in both our experiment and theoretical calculations follows with a rapid decrease in the  $c/a$  ratio.<sup>19</sup> This suggests that the evolution of bulk superconductivity and the Eu valence change do not occur simultaneously, and instead the change in valence behavior above 9 GPa could well be correlated to the structural change from the orthorhombic to the collapsed tetragonal phase reported in literature.<sup>18,19</sup> In addition, the magnetic transition reported under compression<sup>21</sup> occurs around similar pressure range.

The calculated electron density of states (DOS) for  $\text{EuFe}_2\text{As}_2$  is shown in Figure 2(c). For tetragonal  $\text{EuFe}_2\text{As}_2$ , we have obtained A-type anti-ferromagnetic ordering of Eu. The calculated magnetic moment of Eu is  $6.995 \mu\text{B}$ . In the figure, we see that the Eu 4f states form a localized peak 2.7 eV below the Fermi level at ambient pressure. As the pressure increases to 30 GPa, the 4f peak shifts to higher energy state but is still 2 eV below the Fermi level. Furthermore, our theoretical calculations show survival of antiferromagnetic ordering at high pressures above 8 GPa.<sup>20,23</sup> The magnetic moment increases slightly to  $7.012 \mu\text{B}$  at 40 GPa. These changes are not associated with the typical trivalent Eu state in  $\text{EuN}$  and  $\text{EuP}$ , which is characterized by lower magnetic moments and an empty f-state sitting very close to the Fermi level.<sup>24</sup> In the case of  $\text{EuFe}_2\text{As}_2$ , the occupied Eu f-states are deeper in the valence band. The 3d-states of Fe are dominant in both conduction band and valence band edge. Therefore, it is energetically unfavorable to transfer one f-electron to satisfy the trivalency of the Eu ion. The calculated f-electron charge decrease is less than  $0.02 e^-/\text{Eu}$  from 0 to 30 GPa. Nevertheless, we obtain a charge increase of the projected d-electron charge of Eu from 0.416 to  $0.832 e^-/\text{Eu}$ , corresponding to a net magnetic moment increase from 0.090 to  $0.146 \mu\text{B}$ . As a result, a

plausible cause for the divalent-trivalent transition could be the transfer and delocalization of the d-state electrons of Eu. In addition, a slight 4f-delocalization and increased Eu 4f-Fe 3d hybridization can be seen in the high pressure DOS plot, which may also promote the valence transition. In summary, the valence state of Eu has been investigated in  $\text{EuFe}_2\text{As}_2$  at low temperatures and high pressures up to 43 GPa at 10 K. A valence transition from the divalent state to a nearly trivalent state has been observed under compression. The experimental results are consistent with theoretical calculations.

Portions of this work were performed at HPCAT (Sector 16), Advanced Photon Source (APS), Argonne National Laboratory. HPCAT is supported by CIW, CDAC, UNLV, and LLNL through funding from DOE-NNSA, DOE-BES, and NSF. APS is supported by DOE-BES, under Contract No. DE-AC02-06CH11357. The UNLV High Pressure Science and Engineering Center was supported by the U.S. Department of Energy, National Nuclear Security Administration, under Co-operative Agreement No. DE-NA0001982. RSK would like to acknowledge GSECARS/COMPRESS for the use of gas loading system and Sergey Tkachev for technical help. RSK also would like to thank Curtis Benson HPCAT for help setting up the cryostat.

<sup>1</sup>Y. Kamihara, T. Watanabe, M. Hirano, and H. Hosono, *J. Am. Chem. Soc.* **130**, 3296 (2008).

<sup>2</sup>H. Wen, G. Mu, L. Fang, H. Yang, and X. Zhu, *Europhys. Lett.* **82**, 17009 (2008).

<sup>3</sup>M. S. Torikachvili, S. L. Budko, N. Ni, and P. C. Canfield, *Phys. Rev. Lett.* **101**, 057006 (2008).

<sup>4</sup>P. L. Alireza, Y. T. Chris Ko, J. Gillett, C. M. Petrone, J. M. Cole, G. G. Lonzarich, and S. E. Sebastian, *J. Phys. C* **21**, 012208 (2009).

<sup>5</sup>C. F. Miclea, M. Nicklas, H. S. Jeevan, D. Kasinathan, Z. Hossain, H. Rosner, P. Gegenwart, C. Geibel, and F. Steglich, *Phys. Rev. B* **79**, 212509 (2009).

<sup>6</sup>T. Terashima, N. Kurita, A. Kikkawa, H. S. Suzuki, T. Matsumoto, K. Murata, and S. Uji, *J. Phys. Soc. Jpn.* **79**, 103706 (2010).

<sup>7</sup>H. S. Jeevan, Z. Hossain, D. Kasinathan, H. Rosner, C. Geibel, and P. Gegenwart, *Phys. Rev. B* **78**, 052502 (2008).

<sup>8</sup>Z. Ren, Z. Zhu, S. Jiang, X. Xu, Q. Tao, C. Wang, C. Feng, G. Cao, and Z. Xu, *Phys. Rev. B* **78**, 052501 (2008).

<sup>9</sup>Y. Xiao, J. Su, M. Mevan, R. Mittal, C. M. N. Kumar, T. Chatterji, S. Price, J. Person, N. Kumar, S. K. Dhar, A. Thamizhavel, and T. Brueckel, *Phys. Rev. B* **80**, 174424 (2009).

<sup>10</sup>J. Herrero-Martin, V. Scagnoli, C. Mazzoli, Y. Su, R. Mittal, Y. Xiao, T. Brueckel, N. Kumar, S. K. Dhar, A. Thamizhavel, and L. Paolasini, *Phys. Rev. B* **80**, 134411 (2009).

<sup>11</sup>C. Dallera, E. Anese, J.-P. Rueff, A. Palenzona, G. Vanko, L. Braicovich, A. Shukla, and M. Grioni, *Phys. Rev. B* **68**, 245114 (2003).

<sup>12</sup>R. S. Kumar, A. Svane, G. Vaitheeswaran, V. Kanchana, E. D. Bauer, M. Hu, M. F. Nicol, and A. L. Cornelius, *Phys. Rev. B* **78**, 075117 (2008).

<sup>13</sup>R. S. Kumar, A. Svane, G. Vaitheeswaran, Y. Zhang, V. Kanchana, M. Hofmann, S. J. Campbell, Y. Xiao, P. Chow, C. Chen, Y. Zhao, and A. L. Cornelius, *Inorg. Chem.* **52**, 832 (2013).

<sup>14</sup>J. P. Perdew and A. Zunger, *Phys. Rev. B* **23**, 5048 (1981).

<sup>15</sup>A. Svane, *Phys. Rev. B* **53**, 4275 (1996).

<sup>16</sup>W. M. Temmerman, A. Svane, Z. Szotek, H. Winter and S. Beiden, in *Electronic Structure and Physical Properties of Solids: The Uses of the LMTO Method*, Lecture Notes in Physics Vol. 535, edited by H. Dreyssé (Springer-Verlag, Berlin, 2000), pp. 286–312.

<sup>17</sup>O. K. Andersen, *Phys. Rev. B* **12**, 3060 (1975).

<sup>18</sup>W. Uhoya, G. Tsoi, Y. K. Vohra, M. A. McGuire, A. S. Sefat, B. C. Sales, D. Mandrus, and S. T. Weir, *J. Phys.: Condens. Matter* **22**, 292202 (2010).

<sup>19</sup>W. O. Uhoya, G. M. Tsoi, Y. K. Vohra, M. A. McGuire, and A. S. Sefat, *J. Phys.: Condens. Matter* **23**, 365703 (2011).

<sup>20</sup>N. Kurita, M. Kimata, K. Kodama, A. Harada, M. Tomita, H. S. Suzuki, T. Matsumoto, K. Murata, S. Uji, and T. Terashima, *Phys. Rev. B* **83**, 214513 (2011).

<sup>21</sup>J. Paglione and R. L. Greene, *Nature* **6**, 645 (2010).

<sup>22</sup>L. Sun, J. Guo, G. Chen, X. Chen, X. Dong, W. Lu, C. Zhang, Z. Jiang, Y. Zou, S. Zhang, Y. Huang, Q. Wu, X. Dai, Y. Li, J. Liu, and Z. Zhao, *Phys. Rev. B* **82**, 134509 (2010).

<sup>23</sup>K. Matsubayashi, M. Hedo, I. Umehara, N. Katayama, K. Ohgushi, A. Yamada, K. Munakata, T. Matsumoto, and Y. Uwatoko, *J. Phys.: Conf. Ser.* **215**, 012187 (2010).

<sup>24</sup>M. Horne, P. Strange, W. M. Temmerman, Z. Szotek, A. Svane, and H. Winter, *J. Phys.: Condens. Matter* **16**, 5061 (2004).